

# Development of Hyperactivity after Hearing Loss in a Computational Model of the Dorsal Cochlear Nucleus Depends on Neuron Response Type

Roland Schaette<sup>1,2,3</sup> and Richard Kempster<sup>1,2,3,4</sup>

Affiliations: <sup>1</sup> Institute for Theoretical Biology  
Department of Biology  
Humboldt-Universität zu Berlin  
Invalidenstr. 43  
10115 Berlin, Germany  
<sup>2</sup> Bernstein Center for Computational Neuroscience Berlin  
Philippstr. 13  
10115 Berlin, Germany  
<sup>3</sup> Neuroscience Research Center  
Charité, Univeritätsmedizin Berlin  
Campus Charité Mitte  
Charité-Platz 1  
10117 Berlin, Germany  
<sup>4</sup> NeuroCure-Center for Neurosciences Berlin

Final version, accepted for publication in Hearing Research.

## Abstract

Cochlear damage can change the spontaneous firing rates of neurons in the dorsal cochlear nucleus (DCN). Increased spontaneous firing rates (hyperactivity) after acoustic trauma have been observed in the DCN of rodents such as hamsters, chinchillas and rats. This hyperactivity has been interpreted as a neural correlate of tinnitus. In cats, however, the spontaneous firing rates of DCN neurons were not significantly elevated after acoustic trauma. Species-specific spontaneous firing rates after cochlear damage might be attributable to differences in the response types of DCN neurons: In gerbils, type III response characteristics are predominant, whereas in cats type IV responses are more frequent. To address the question of how the development of hyperactivity after cochlear damage depends on the response type of DCN neurons, we use a computational model of the basic circuit of the DCN. By changing the strength of two types of inhibition, we can reproduce salient features of the responses of DCN neurons. Simulated cochlear damage, which decreases the activity of auditory nerve fibers, is assumed to activate homeostatic plasticity in projection neurons (PNs) of the DCN. We find that the resulting spontaneous firing rates depend on the response type of DCN PNs: PNs with type III and type IV-T response characteristics may become hyperactive, whereas type IV PNs do not develop increased spontaneous firing rates after acoustic trauma. This theoretical framework for the mechanisms and circumstances of the development of hyperactivity in central auditory neurons might also provide new insights into the development of tinnitus.

## Introduction

Hearing loss through cochlear damage can lead to the development of increased spontaneous firing rates (hyperactivity) in the dorsal cochlear nucleus (DCN; Kaltenbach and McCaslin, 1996). Damage to cochlear hair cells through acoustic trauma (Kaltenbach et al., 1998) and loss of outer hair cells after cisplatin administration (Kaltenbach et al., 2002) lead to similar increases in the spontaneous firing rates, indicating that hyperactivity develops as a response to impaired cochlear function. Furthermore, increased spontaneous firing rates of DCN neurons are related to behavioral evidence of tinnitus (Brozoski et al., 2002; Kaltenbach et al., 2004).

The change of spontaneous firing rates in the DCN after acoustic trauma, however, depends on the species and the preparation. In chinchillas, increased spontaneous firing rates were recorded from putative fusiform cells, the principal neurons of the DCN (Brozoski et al., 2002, anesthetized animals). In hamsters and rats, hyperactivity was observed in extracellular recordings from the surface of the DCN (Kaltenbach and McCaslin, 1996; Kaltenbach et al., 2004; Kaltenbach and Zhang, 2007, anesthetized animals). In cats, on the other hand, spontaneous firing rates in the DCN were not significantly different from control levels (Ma et al., 2006, decerebrate preparation). It is unclear why the occurrence and characteristics of hyperactivity differ from species to species.

Neurons in the DCN show a variety of complex responses to pure-tone and noise stimuli. The most diverse response characteristics have been recorded from the DCN's principal cells. Their responses range from 'type III', with monotonic rate-intensity functions for pure tone and noise stimuli, to 'type IV', which are characterized by strongly non-monotonic responses to pure tones (see Young and Davis, 2002, for a review). Interestingly, the predominant response type differs between species. In cats, mostly type IV responses are recorded from principal cells (decerebrate preparation, Young, 1980), whereas in gerbils type III response properties are most abundant (decerebrate preparation, Davis et al., 1996b; Ding et al., 1999), which might also be true for other rodent species such as chinchillas and hamsters. These differences could indicate species-specific tuning of the computational properties of the DCN, which might lead to differences in the adaptation to altered activity statistics of the auditory nerve (AN) induced by hearing loss.

Principal cells of the DCN receive excitatory input from the ipsilateral AN, inhibitory input from interneurons, and input from other sources like the somatosensory system (see, e.g., Davis et al., 1996b; Young and Davis, 2002; Shore, 2005). They project to the inferior colliculus, forming the output of the DCN. To account for the response properties of these DCN projection neurons (PNs), a minimal circuit has been proposed (see, e.g., Young and Davis, 2002), where a PN is inhibited by two types of interneurons: type II and wide-band inhibitor (WBI) neurons. Both interneurons also receive excitation from the ipsilateral AN. The type II neuron has a best frequency that is close to the PN's best frequency, and it inhibits the PN's response to pure tones or other narrow-band stimuli of high enough intensity. The WBI neuron, on the other hand, strongly responds to broad-band noise, but only weakly to pure tones. It is assumed to inhibit DCN projection neurons as well as type II neurons. Modeling results show that the different response types of DCN principal cells can be reproduced with this circuit by adjusting the strengths of the inhibitory inputs to the PNs (Zheng and Voigt, 2006b).

Recently, we have proposed a computational model that links the development of hyperactivity after hearing loss to activity regulation through homeostatic plasticity (Schaette and Kempster, 2006). Homeostatic plasticity is a mechanism that stabilizes the mean activity of neu-

rons by scaling the strength of excitatory and inhibitory synapses and by adjusting the intrinsic excitability (see Turrigiano, 1999, for a review). When excitatory synapses are strengthened and the excitability is increased to compensate for decreased AN activity after hearing loss, the spontaneous firing rates of cochlear nucleus neurons can be increased (Schaeffer and Kemper, 2006). This model contained only excitatory connections, and therefore it cannot account for the differences in the response types of DCN principal cells described above. Here we incorporate the basic neuronal circuit of the DCN into the model. By varying the connection strengths, we are able to reproduce essential features of the various response types of DCN neurons. For each response type, we determine the impact of hearing loss, and we evaluate the effects of a homeostatic stabilization of the mean firing rate. We find that the development of hyperactivity strongly depends on the PN response type, which could explain controversial experimental results on hyperactivity in the DCN after acoustic trauma.

## Methods

We set up a phenomenological model of the responses of AN fibers and DCN neurons. The model is phrased in terms of firing rates of small populations of AN fibers and DCN neurons, similar to the model used in Schaette and Kempner (2006).

### Distribution of Sound Intensities in the Acoustic Environment

A typical acoustic environment consists of a mixture of various sounds, like for example speech, animal vocalizations, environmental sounds, and noise. We assume that the probability density function  $p_I(I)$  of the sound intensity levels  $I$  (in units of dB) is Gaussian (Fig. 1a, top panel). Based on values from the literature (Escabi et al., 2003; Christopher Kirk and Smith, 2003; Singh and Theunissen, 2003), we choose a mean intensity of 40 dB and a standard deviation of 25 dB for all frequency channels.

### Auditory-Nerve Model

The AN model used in this study is organized in frequency channels. We consider four frequency channels per octave. Each frequency channel comprises type I AN fibers with similar characteristic frequencies, but different thresholds and spontaneous discharge rates. The response of such a small population of AN fibers in each frequency channel is described by a population firing rate  $f(I)$ , which is an average over many fibers:

$$f(I) = \begin{cases} f_{\text{sp}} & \text{for } I < I_{\text{th}}, \\ f_{\text{sp}} + (f_{\text{max}} - f_{\text{sp}}) \frac{\int_{I_{\text{th}}}^I dI' p_I(I')}{1 - P_{\text{sp}}} & \text{for } I \geq I_{\text{th}}. \end{cases} \quad (1)$$

The response threshold of the AN fiber population is set to  $I_{\text{th}} = 0$  dB SPL, which corresponds to the threshold of the most sensitive AN fibers. For sub-threshold stimuli, there is spontaneous activity at  $f_{\text{sp}} = 50$  Hz. For supra-threshold stimuli, the firing-rate response grows with increasing sound intensity and saturates at a maximum firing rate of  $f_{\text{max}} = 250$  Hz (Fig. 1a, central panel). For simplicity, we choose  $f(I)$  to be proportional to the integral of the intensity distribution  $p_I(I)$ , so that  $f$  has maximum information on  $I$  for  $I > I_{\text{th}}$  (infomax principle, see Laughlin, 1981).  $P_{\text{sp}}$  denotes the probability of spontaneous activity, which is given by  $P_{\text{sp}} = \int_{-\infty}^{I_{\text{th}}} dI p_I(I)$ .

From the sound intensity distribution  $p_I(I)$  and the rate-intensity function  $f(I)$ , we can derive the probability distribution  $p_f(f)$  of the firing rates of our model AN fibers in each frequency channel (Fig. 1a, right panel).  $p_f(f)$  has a delta peak at  $f = f_{\text{sp}} = 50$  Hz, as spontaneous activity occurs with a probability of  $P_{\text{sp}} = 0.05$ . The probability density  $p_d = (1 - P_{\text{sp}})/(f_{\text{max}} - f_{\text{sp}})$  of responses evoked by supra-threshold sounds ( $50 \text{ Hz} < f \leq 250 \text{ Hz}$ ) is constant, because we assumed that the AN rate-intensity function is tuned to the distribution of sound intensities. In total, we have

$$p_f(f) = P_{\text{sp}} \delta(f - f_{\text{sp}}) + \begin{cases} p_d & \text{for } f_{\text{sp}} < f \leq f_{\text{max}} \\ 0 & \text{otherwise.} \end{cases} \quad (2)$$

The mean rate  $\langle f \rangle$  of the AN fiber population is then given by  $\langle f \rangle = \int df' f' \cdot p_f(f')$ , and, because of the simplifying assumptions, we obtain the expression

$$\langle f \rangle = P_{\text{sp}} f_{\text{sp}} + \frac{1}{2} (1 - P_{\text{sp}}) (f_{\text{max}} + f_{\text{sp}}). \quad (3)$$

For the parameters we chose to describe responses from a healthy cochlea, the mean firing rate for the AN fiber population of each frequency channel is 145 Hz.

## AN Responses to Pure-Tone and Noise Stimuli

Responses to pure-tone stimuli are captured by varying the sound intensity in one frequency channel, which leads to a firing rate response according to Eq. (1) in the corresponding AN fiber population. The AN fibers of all other frequency channels remain at their spontaneous rate. For broad-band noise, the sound intensity is set to the same value in all frequency channels. Consequently, the AN fiber populations of all frequency channels fire at the same rate in response to broad-band noise.

## Effects of Hearing Loss on AN Activity

Hearing loss through cochlear damage alters the response properties of auditory nerve fibers. We model the effects of inner hair cell (IHC) loss, outer hair cell (OHC) loss, and noise-induced damage to the stereocilia of IHCs and OHCs (stereocilia damage, SD) by altering the AN rate-intensity functions.

Isolated loss of IHCs can be induced by the administration of carboplatin (Wang et al., 1997; McFadden et al., 1998). After IHC loss, the compound action potential of the AN is reduced in proportion to the amount of IHC loss, whereas the response threshold remains unaffected (Wang et al., 1997). To capture these changes in our model, we scale down the AN population response (Fig. 1b, top panel).

Administration of cisplatin or gentamycin can lead to pure loss of OHCs (Dallos and Harris, 1978; Kaltenbach et al., 2002), which increases the response threshold of AN fibers, but does not alter the spontaneous and maximum discharge rates (Dallos and Harris, 1978). We model OHC loss by increasing the response threshold  $I_{\text{th}}$  of the AN population response in proportion to the amount of OHC loss, with an increase of the threshold by 60 dB for complete loss of OHCs (Fig. 1b, middle panel). The spontaneous rate  $f_{\text{sp}}$  and the maximum rate  $f_{\text{max}}$  remain unaffected.

Acoustic trauma damages the stereocilia of IHCs and OHCs and can also lead to hair cell loss (Kaltenbach et al., 1992; Wang et al., 2002). Typically, noise-induced stereocilia damage increases the response threshold and decreases the spontaneous firing rate of the affected AN fibers, whereas the maximum firing rate remains constant (Lieberman and Dodds, 1984; Liberman and Kiang, 1984). For simplicity, we consider only the common case where the stereocilia of inner and outer hair cells are damaged to a similar degree. To simulate this kind of SD, we increase the response threshold  $I_{\text{th}}$  up to 80 dB, and decrease the spontaneous firing rate  $f_{\text{sp}}$  up to a factor of 2/3. The maximum rate  $f_{\text{max}}$  is not altered (Fig. 1b, bottom panel).

Inserting the altered values for threshold, spontaneous, and maximum firing rate into equation (1) yields the responses of the AN fiber population after cochlear damage (Fig. 1b). The

mean rate of the AN can be calculated by adjusting the values of  $I_{\text{th}}$ ,  $f_{\text{sp}}$ ,  $f_{\text{max}}$ , and  $P_{\text{sp}}$  in equations (2), and (3) to the values for a certain type of cochlear damage (see Schaette and Kempter, 2006, for more details).

## Model for Wide-Band Inhibitor Neurons

In the basic DCN circuit as proposed by Young and coworkers (see, e.g., Young and Davis, 2002), the WBI neuron receives only excitatory input from AN fibers. Our model WBI neuron receives input from the AN fiber populations of several frequency channels (see Fig. 2a). This WBI neuron has a simple threshold-linear response function  $W$  with a firing threshold  $\theta_w$ . The firing rate  $w$  of the WBI neuron in response to AN input from  $N$  frequency channels firing at rates  $f_1, \dots, f_N$  is

$$w = W(f_1, f_2, \dots, f_N) = \left[ \frac{1}{N} \sum_{i=1}^N f_i - \theta_w \right]_+, \quad (4)$$

where  $[\dots]_+$  denotes positive rectification. Here we consider input from  $N = 10$  different AN frequency channels whose characteristic frequencies (CFs) span 2.5 octaves. Moreover, we set the firing threshold to  $\theta_w = 100$  Hz. The resulting WBI model neuron is not spontaneously active, and it does not respond to pure tones. It has a monotonic rate-intensity function for broad-band noise with a response threshold of 27 dB, which is the noise intensity  $I$  needed to evoke an AN response of  $f(I) = \theta_w$  (Fig. 2b). Cochlear damage thus increases the response threshold of the WBI neuron.

We assume that the firing rates of AN fibers from different frequency channels are mutually independent, which is of course an oversimplification but a feasible approximation to obtain the firing rate distribution  $p_w(w)$  of the WBI neuron from the response distributions of the afferent AN fibers in a two-step process: First, we derive the probability distribution  $p_s(s)$  of the synaptic input  $s = \sum f_i/N$  by convolving the firing rate distributions  $p_{f_1}, \dots, p_{f_N}$  of all afferent AN frequency channels and scaling by the synaptic weight factor:

$$\begin{aligned} p_s(s) &= N \cdot (p_{f_1} * \dots * p_{f_N})(s \cdot N) \\ &= N \cdot \int_{-\infty}^{\infty} df_1 p_{f_1}(f_1) \dots \int_{-\infty}^{\infty} df_{N-1} p_{f_{N-1}}(f_{N-1}) \int_{-\infty}^{\infty} df_N p_{f_N}(s \cdot N - f_1 - \dots - f_{N-1}) \end{aligned} \quad (5)$$

The convolution is carried out numerically. Second, we apply the response threshold  $\theta_w$  to the input distribution  $p_s(s)$ . We find that the WBI neuron does not fire with probability  $P_0 = \int_0^{\theta_w} ds p_s(s)$ , and its response distribution is

$$p_w(w) = P_0 \delta(w) + \begin{cases} p_s(w + \theta_w) & \text{for } 0 < w \leq w_{\text{max}} \\ 0 & \text{otherwise,} \end{cases} \quad (6)$$

where  $w_{\text{max}} = f_{\text{max}} - \theta_w$  is its maximum firing rate (with  $f_{\text{max}}$  being the maximum firing rate of the AN fibers). In the healthy case, the resulting firing rate distribution of the model WBI neuron resembles a Gaussian distribution, plus a delta peak at 0 Hz, as the WBI neuron is inactive with probability 0.009 (Fig. 2c). The mean rate  $\langle w \rangle$  of the WBI neuron is then given

by

$$\langle w \rangle = \int dw w p_w(w), \quad (7)$$

and we obtain a mean rate of 45 Hz for AN input from an undamaged cochlea.

## Model for Narrow-Band Inhibitor Neurons

Our model for a narrow-band inhibitor (NBI) neuron of the DCN is based on the response properties that have been reported for type II neurons (see Young and Davis, 2002, for a review). The model NBI neuron receives excitation from AN fibers of a single frequency channel, and it is inhibited by a WBI neuron. For simplicity, we assume that the NBI neuron and the WBI neuron receive input from different AN frequency channels (Fig. 3a).

From our assumption of independent AN frequency channels (see above), it follows that the firing rate  $f$  of the NBI neuron's afferent AN fiber population and the firing rate  $w$  of the WBI neuron are also mutually independent. This independence assumption provides a feasible approximation of the relation between AN and WBI input. The general case with a stimulus-dependent relation between the two is much more difficult to handle, and the degree of dependence is sensitive to the kind of stimuli chosen to represent a natural acoustic environment. Even in a natural acoustic environment we expect only a weak correlation between the activity of AN fibers driving a DCN type II neuron and the activity of WBI neurons inhibiting this type II neuron, as WBI neurons have very large receptive fields.

It is assumed that the NBI neuron has a threshold-linear response function  $N$  with a firing threshold  $\theta_n$ . Its firing rate  $n$  in response to AN input at rate  $f$  and WBI input at rate  $w$  is given by

$$n = N(f, w) = [g_f f - g_{nw} w - \theta_n]_+, \quad (8)$$

where the gain factor  $g_{nw}$  determines the strength of the inhibition from the WBI neuron. We set  $g_{nw} = 1.5$  and use  $\theta_n = \theta_w = 100$  Hz for the firing thresholds, so that the NBI neuron is inhibited by broad-band noise. The gain factor  $g_f$  for excitation from the AN is set to one without loss of generality. Both gain factors and the firing thresholds remain fixed, i.e. they are not regulated by homeostatic plasticity, as we only consider homeostatic plasticity in PNs in our model. The resulting response threshold of the NBI neuron for stimulation with pure tones is 27 dB, which is the intensity  $I$  needed to evoke an AN response of  $f(I) = \theta_n$ . The NBI neuron has a monotonic rate-intensity function for pure tones (Fig. 3b), and it does not respond to broad-band noise.

Because we have assumed that  $f$  and  $w$  are independent in our idealized acoustic environment, their joint probability distribution factorizes,  $p(f, w) = p_f(f)p_w(w)$ . The mean rate  $\langle n \rangle$  of the NBI neuron is then given by

$$\langle n \rangle = \int \int_{f w} dw df p_f(f) p_w(w) N(f, w). \quad (9)$$

For the healthy case, we obtain a mean rate of 19 Hz (Fig. 3c).

The response distribution  $p_n(n)$  of the NBI neuron can be derived from  $p_w$  and  $p_f$  and equation (8) with  $g_f = 1$ . As a first step, we consider the distribution  $p_s$  of the NBI neuron's

effective synaptic input  $s := f - g_{\text{nw}}w$ ,

$$p_s(s) = \int df \int dw p_f(f) p_w(w) \delta(s - f + g_{\text{nw}}w). \quad (10)$$

By substituting  $w$  with  $w' = g_{\text{nw}}w$ , where  $p_{w'}(w') = p_w(w'/g_{\text{nw}})/g_{\text{nw}}$ , we obtain

$$p_s(s) = \int df p_f(f) p_{w'}(f - s). \quad (11)$$

Applying the NBI neuron's firing threshold  $\theta_n$  then yields the distribution  $p_n$  of its firing rate responses:

$$p_n(n) = P_0 \delta(n) + \begin{cases} p_s(n + \theta_n) & \text{for } 0 < n \leq n_{\text{max}} \\ 0 & \text{otherwise} \end{cases} \quad (12)$$

The NBI neuron does not fire with probability  $P_0 = \int_0^{\theta_n} ds p_s(s)$ , and  $n_{\text{max}} = f_{\text{max}} - \theta_n$  is its maximum firing rate. The resulting response distribution for an undamaged cochlea is shown in Fig. 3c. This distribution has a delta peak at 0 Hz, as the NBI neuron is inactive with probability 0.6.

## Model for Projection Neurons

In our model for a projection neuron (PN) of the DCN, we consider excitation by AN fibers from a single frequency channel, and inhibition from a WBI and a NBI neuron (Fig. 4a). We assume that the NBI neuron receives excitatory input from AN fibers of the same frequency channel as the PN, and that both the PN and the NBI neuron are inhibited by the same WBI neuron. Our model neurons represent small populations of real neurons. In this way, we approximate the situation in the DCN, where PNs and type II neurons each receive inhibition from WBI neurons with similar characteristics, but not necessarily from the same neurons.

The strength of the inhibitory projection from the WBI neuron onto the PN is quantified by the gain factor  $g_w$ , and the efficacy of inhibition from the NBI neuron is determined by the gain factor  $g_n$ . The gain factor  $g_f$  for input from the AN to the PN is set to  $g_f = 1$  without loss of generality. For the response function  $R$  of the PN, we choose a hyperbolic tangent with positive rectification, as this is a saturating function with convenient analytical properties. With a response threshold of 0 Hz, the PN's firing rate  $r$  is given by

$$r = R(f, w) = r_{\text{high}} \tanh \left( [g_f f - g_w w - g_n N(f, w)]_+ / r_{\text{high}} \right) \quad (13)$$

where  $f$  is the firing rate of the afferent AN fiber population,  $w$  is the firing rate of the WBI neuron, and  $r_{\text{high}} = 300$  Hz is the maximum possible firing rate of the PN. The firing rate of the NBI neuron is  $N(f, w)$  with the same  $f$  and  $w$  as the PN's direct input from the AN and WBI neuron.

We assume that  $f$  and  $w$  are mutually independent, as already discussed for the NBI neuron. The mean firing rate  $\langle r \rangle$  of the PN can then be calculated numerically according to

$$\langle r \rangle = \iint_{f w} dw df p_f(f) p_w(w) R(f, w), \quad (14)$$

which depends on the gain factors  $g_w$  and  $g_n$  (Fig. 5), and on the status of the cochlea. The probability distribution of the PN's responses is also determined numerically (Fig. 6a).

## Homeostatic Plasticity in Projection Neurons

We assume that the mean firing rates  $\langle r \rangle$  of DCN projection neurons are stabilized by homeostatic plasticity at a certain target rate  $r^*$ . For each PN type, i.e. each combination of the gain parameters  $g_w$  and  $g_n$ , the target firing rate  $r^*$  is set to the mean firing rate obtained for input from healthy AN fibers (Fig. 5). In this model, we consider homeostasis through global scaling of synapse strengths (Turrigiano, 1999). Scaling is implemented through the homeostasis factor  $h$ , which alters the gain of excitatory and inhibitory inputs in a multiplicative fashion. The gain of excitatory inputs is multiplied with  $h$ , and the gain of inhibitory inputs is divided by  $h$  to emulate the opposite regulation of the strengths of excitatory and inhibitory inputs, as observed in experiments (Turrigiano et al., 1998; Kilman et al., 2002). In the healthy case, we have  $h = 1$ . The value of the homeostasis factor is limited to the range of  $[0.3, 3]$  to account for physiological constraints on synaptic strength and neuronal excitability (see Discussion). The response  $r$  of a PN in dependence upon the value of the homeostasis factor  $h$  is then

$$r = R(f, w, h) = r_{\text{high}} \tanh \left( \left[ h \cdot f - \frac{g_w}{h} w - \frac{g_n}{h} N(f, w) \right]_+ / r_{\text{high}} \right). \quad (15)$$

When the mean rate  $\langle r \rangle$  of a PN is decreased below  $r^*$ , the factor  $h$  is increased until the mean rate is restored. An increase in  $h$  strengthens excitatory and weakens inhibitory projections onto the PN and thus increases its mean firing rate. Similarly, if  $\langle r \rangle$  is increased above  $r^*$ ,  $h$  is decreased. The exact value of  $h$  that is necessary to adjust the PN's mean firing rate to the target level is determined numerically.

## Additional Acoustic Stimulation

When an acoustic stimulus is presented at an intensity  $I_{\text{stim}}$  that exceeds the response threshold  $I_{\text{th}}$ , the corresponding AN fibers fire at rate  $f_{\text{stim}} = f(I_{\text{stim}})$ . For continuous stimulus presentation in addition to the acoustic environment, the spontaneous AN firing rate  $f_{\text{sp}}$  is thus replaced by  $f_{\text{stim}}$ , which occurs with probability  $P_{\text{stim}} = \int_{-\infty}^{I_{\text{stim}}} dI p_I(I)$ , i.e. whenever  $I_{\text{stim}}$  is higher than the intensity  $I$  of an environmental stimulus with distribution  $p_I$ . To calculate the mean firing rates of AN fibers and DCN neurons with additional acoustic stimulation, we thus take the altered AN response distributions into account by replacing  $P_{\text{sp}}$  by  $P_{\text{stim}}$  and  $f_{\text{sp}}$  by  $f_{\text{stim}}$ . If this raises the mean firing rate of a DCN PN above the target value  $r^*$ , homeostatic plasticity lowers  $h$ . Decreasing  $h$  can reduce hyperactivity. 'Anti-hyperactivity' stimuli are derived in an iterative process by adjusting the stimulus intensities in each frequency channel such that after the stimulus is turned off, the spontaneous firing rates of the PNs under study are close to the healthy spontaneous firing rates.

The model was implemented using MATLAB from the MathWorks Inc., Natick, Massachusetts.

## Results

In this study, we focus on the question of how altered sensory input and homeostatic plasticity change the spontaneous firing rates of neurons. In particular, we investigate under which circumstances sensorineural hearing loss leads to hyperactivity of projection neurons (PNs) in the dorsal cochlear nucleus (DCN), and how hyperactivity depends on the PN's response type. In the Methods section, we have set up a phenomenological model for the responses and activity statistics of auditory nerve (AN) fibers and DCN neurons. The model for PNs is based on the minimal circuit that has been proposed for the DCN (see Young and Davis, 2002, for a review), where PNs are inhibited by wide-band inhibitor (WBI) and type II neurons (Fig. 4a). We call the type II neurons narrow-band inhibitor (NBI) neurons, referring to their function of providing inhibition to a PN for narrow-band stimuli only (Young and Davis, 2002). WBI, NBI, and projection neurons receive excitation from the ipsilateral AN. Moreover, NBI neurons also receive inhibition from WBI neurons. For simplicity, here we do not consider additional or non-auditory inputs to DCN PNs (Schaette and Kempner, 2006); see also Discussion.

We adjust the connection strengths in the basic DCN circuit such that salient features of the responses of DCN principal cells are reproduced. For different sets of connection strengths, we then evaluate the effects of hearing loss on the activity of the DCN model neurons, and determine the consequences of activity-dependent plasticity in PNs.

### Responses of Projection Neurons to Tone- and Noise-Stimuli

The responses of the model PNs to tone and noise stimuli are determined by two gain factors of inhibitory input:  $g_w$  for the WBI neuron and  $g_n$  for the NBI neuron (Fig. 4a). All other connection strengths and response thresholds remain fixed at values that produce response characteristics of NBI and WBI neurons. The strength of the excitatory connection from the AN to the PN is initially set to one without loss of generality (see Methods for details).

When both  $g_w$  and  $g_n$  are set to low values, for example  $g_w = 0.6$  and  $g_n = 0.5$  in Fig. 4b, the PN exhibits monotonic rate-intensity functions for both pure tones and broad-band noise, resembling the responses of type III neurons of the DCN (see Rhode and Greenberg, 1992; Young and Davis, 2002, for reviews). For  $g_w = 0.6$  and  $g_n = 1.3$  in Fig. 4c, the PN's rate-intensity function for pure tones becomes non-monotonic: pure tones at low and medium intensities excite the PN, whereas for pure tones at high sound intensities, its response is close to the spontaneous rate. We furthermore observe an excitatory, monotonic response to noise. Such response properties resemble type IV-T neurons of the DCN (Davis et al., 1996a; Ding et al., 1999). Increasing both  $g_w$  and  $g_n$  even further, we can change the responses of the model PN to resemble type IV characteristics (Young and Davis, 2002). An example for  $g_w = 1.1$  and  $g_n = 3$  is shown in Fig. 4d: The responses to pure tones are strongly non-monotonic, and the PN is inhibited already at medium sound intensities. The responses to broad-band noise are also non-monotonic, but they are still excitatory at all sound intensities.

### Mean Firing Rates of the Projection Neurons

The different response types of DCN PNs are characterized by different mean firing rates (which are stabilized by homeostatic plasticity, see below). We note that the mean activity of a PN depends on the activity statistics of the inputs as well as on the efficacy of its exci-

tatory and inhibitory inputs. In our feedforward network of the DCN, the activity statistics of model neurons can be derived from the activity statistics of the afferent AN fibers, which are determined by the acoustic environment and their rate-intensity functions (Fig. 1).

How the mean rate of a PN depends on the strengths  $g_w$  and  $g_n$  of inhibition from WBI and NBI neurons is shown in Fig. 5 for an undamaged cochlea. Increasing  $g_w$  or  $g_n$  decreases the mean firing rate of the PN, and we find that  $g_w$  has a stronger influence on the mean firing rate of the PN than  $g_n$ . For high values of  $g_w$ , the mean rate of the PN can be even below the spontaneous rate. The three different response types of DCN projection neuron are depicted in the  $g_w$ - $g_n$  plane by ellipses. The mean rates of PNs with type III and type IV-T response characteristics are more than 1.5 times higher than their spontaneous firing rates, whereas the mean rate of type IV PNs is either slightly above or even below their spontaneous rate.

## Hearing Loss and Homeostatic Plasticity

How are the responses of DCN model neurons altered by different kinds and degrees of cochlear damage, i.e. inner hair cell (IHC) loss, outer hair cell (OHC) loss, and stereocilia damage (SD)? And how does a subsequent stabilization of the mean rate through homeostatic plasticity affect the spontaneous rates of the PNs? To address these questions we assume that homeostatic plasticity stabilizes the activity of PNs by scaling the strength of their afferent excitatory and inhibitory synapses in opposite directions (Turrigiano et al., 1998; Kilman et al., 2002). In our model, this scaling is implemented by means of the homeostasis factor  $h$ : The strength of excitatory synapses onto PNs is multiplied with  $h$ , and the strength of inhibitory synapses onto PNs is divided by  $h$ . In the healthy case, we have  $h = 1$ . When the mean firing rate deviates from its target level,  $h$  is adjusted (see also Methods). For simplicity, we assume that NBI and WBI neurons and their afferent inputs are not affected by homeostatic plasticity. Additional homeostasis in the inhibitory interneurons has only a minor influence on the spontaneous firing rates of PNs (not shown, see Discussion).

We start by analyzing the case where all AN frequency channels are affected by 75% OHC loss. The stabilization of the mean firing rate of a type IV-T model neuron through homeostatic plasticity for this case of OHC loss is illustrated in Fig. 6. OHC loss of 75% increases the response threshold of the AN fiber population by 45 dB, and, consequently, the response threshold of the PN is increased by the same amount. The increased threshold renders many stimuli sub-threshold, and, as a result, the probability of occurrence of spontaneous activity of the PN is increased from 0.005 to 0.38, indicated by a distinct peak in the response distribution at 50 Hz. The mean rate is strongly reduced. We assume that this reduction of the mean rate activates homeostatic plasticity, which increases the strength of excitatory synapses and decreases the strength of inhibitory synapses onto the PN by increasing the homeostasis factor  $h$  from  $h = 1$  to  $h > 1$  (see above and Methods, Eq. 15). In the scenario outlined in Fig. 6c, homeostasis restores the mean rate of the type IV-T PN to its target level, but, as a consequence, also the spontaneous firing rate is increased from 50 Hz to 63 Hz: the neuron finally has become hyperactive.

Stabilization of the mean rate through homeostatic scaling of synapse strengths leads to hyperactivity in our model if the ratio between mean and spontaneous firing rate of a PN is decreased through cochlear damage, i.e. if the mean firing rate is reduced more strongly than the spontaneous firing rate. Therefore, type III and type IV-T neurons (with an initially high ratio of mean and spontaneous firing rates) are more prone to developing hyperactivity after

cochlear damage and homeostatic scaling than type IV neurons (see also Fig. 5).

## **Effects of Cochlear Damage on the AN and the Inhibitory Interneurons**

To understand the differential effects of cochlear damage and homeostasis on the responses of DCN PNs, we take a closer look at all neurons and afferent fibers in the DCN (Fig. 7). We first look at AN activity and summarize the effects of different kinds and degrees of cochlear damage. For simplicity, we assume that the amount of cochlear damage is equal for all frequency channels. As indicated in Fig. 1b, IHC loss scales down the rate-intensity function of the AN's population response, which leads to a reduction of its mean and spontaneous rate in proportion to the degree of IHC loss (Fig. 7, top row, left panel). In contrast, OHC loss was assumed to increase the response threshold of AN fibers, whereas the spontaneous and maximum firing rate remain unchanged. This increase of the response threshold leads to a reduction of the mean AN firing rate, as the probability of stimulus-driven activity is decreased (Fig. 7, top row, middle panel). Finally, noise-induced damage to the stereocilia of inner and outer hair cells was assumed to increase the response threshold and to decrease the spontaneous firing rate of the corresponding AN fibers. Both changes conjointly reduce the mean AN firing rate (Fig. 7, top row, right panel).

The reduction of excitatory drive from the AN after cochlear damage affects WBI, NBI, and projection neurons in our model DCN circuit. In WBI neurons (Fig. 7, second row), the mean firing rate is decreased in proportion to the severity of cochlear damage. When IHC loss exceeds ca. 45% or when SD is more severe than approximately 75%, WBI neurons cease to fire completely.

NBI neurons (Fig. 7, third row) present a more complex case because they receive excitatory input from the AN as well as inhibitory input from WBI neurons: IHC loss reduces the excitatory input to NBI neurons, but they also receive less inhibition due to the decreased activity of the WBI neurons. After mild IHC loss, for example, the mean rate of NBI neurons stays approximately constant. Moderate OHC loss or SD even increase the mean NBI rate because in these cases the reduction of inhibition from WBI neurons outweighs the decrease in excitation from the AN. However, when the mean rate of the AN drops below the firing threshold of the NBI neurons, their mean rate also starts to decline, and when IHC loss exceeds 60%, the NBI neurons cease to fire.

## **Effects of Hearing Loss and Homeostatic Plasticity on Projection Neurons**

The three bottom rows of Figure 7 summarize the effects of cochlear damage and homeostatic plasticity on our three types of PNs (see also Fig. 4b-d). After cochlear damage, these neurons experience not only a reduction of excitatory input from the AN, but also altered inhibition from the interneurons. Homeostatic stabilization of the PNs' mean firing rates further alters their response properties. Although we used a minimal model of DCN responses, the numerically derived response distributions in Figure 7 are rather complex.

The immediate main effect of all kinds of cochlear damage on PNs with type III and type IV-T response characteristics is a reduction of the mean firing rate in proportion to the severity of cochlear damage (not shown; for an example see Fig. 6a,b). In type IV PNs, however, mild IHC loss increases the mean firing rate, whereas severe IHC loss and all degrees of OHC loss and SD lead to a decrease of the mean rate (not shown). We assume that these deviations of the

mean PN firing rates from their target values activate homeostatic plasticity. We now discuss the response distributions of PNs for IHC loss, OHC loss, and SD after homeostatic plasticity has rescaled synapses.

**IHC loss.** Homeostatic plasticity can stabilize the mean rate of our example PNs only up to a certain degree of IHC loss (Fig. 7, left column). For more severe IHC loss, homeostasis is assumed to saturate (at  $h = 3$ , see Methods), and the mean rates decline. The spontaneous firing rates of all PNs remain below their healthy values after homeostatic plasticity. In an earlier model (Schaette and Kempster, 2006), we have shown that the spontaneous firing rates of DCN projection neurons after IHC loss can also depend on the strength of additional excitatory non-auditory inputs. Thus, complete loss of IHCs does not abolish the spontaneous activity of DCN PNs if there is sufficient additional non-auditory input. In the current model, non-auditory inputs were omitted for simplicity, and therefore the PNs cease to fire for complete IHC loss (see Discussion).

**OHC loss.** For all degrees of OHC loss (Fig. 7, middle column), homeostasis is able to restore the mean rates of type III and the type IV-T PNs to their healthy values. In both neuron types, the spontaneous firing rates are increased after homeostasis, as the ratio between mean and spontaneous firing rate was initially decreased by OHC loss. Thus, in our model, OHC loss can lead to hyperactivity in type III and type IV-T PNs. In PNs with type IV response properties, the mean rate is also restored to its target value by homeostasis, regardless of the severity of OHC loss. The spontaneous rate is slightly increased for moderate-to-severe OHC loss. The maximum increase is about 12%, which might be considered strong enough to be detected as hyperactivity.

**Stereocilia damage.** Homeostasis restores the mean firing rates of type III and type IV-T PNs to their target levels up to a critical degree of SD (Fig. 7, right column). The spontaneous firing rates are slightly decreased for mild SD in both PN types, but increased above the healthy level for moderate-to-severe SD. The peak in the curve of spontaneous firing rate versus SD is created by the saturation of homeostasis. In our model for a type IV PN, the mean rate can be stabilized by homeostasis at its target level regardless of the severity of SD. The spontaneous firing rate of the type IV PN, however, remains below its original level after homeostasis.

To further demonstrate how SD and homeostasis change the spontaneous firing rates of DCN PNs, we systematically vary the strength of  $g_w$  and  $g_n$ . Figure 8 displays the spontaneous firing rates of a continuum of PN response characteristics for four degrees of SD (60, 70, 80, and 90%) after homeostasis. For 60% SD, only PNs that receive little inhibition become hyperactive. When cochlear damage is increased, for example to 70-80% SD, the parameter region where hyperactivity is observed becomes larger. At 90% SD, homeostasis is saturated in all PNs receiving low-to-moderate inhibition (lower left corner in the rightmost plot of Fig. 8). Therefore, these neurons have the same spontaneous firing rate.

Figure 8 again demonstrates that PNs with type III and type IV-T response properties can become hyperactive after SD, and that type III neurons are more susceptible to cochlear damage than type IV-T neurons. There is no hyperactivity in the parameter region where type IV responses are obtained. We conclude that in our model SD can cause hyperactivity through homeostatic plasticity in DCN type III and type IV-T PNs, but not in type IV PNs.

## Decreasing Hyperactivity through Additional Acoustic Stimulation

Neuronal hyperactivity in the DCN after hearing loss is correlated to behavioral signs of tinnitus (Brozoski et al., 2002; Kaltenbach et al., 2004). Our model suggests that it might be possible to decrease hyperactivity, and thus probably also tinnitus, through prolonged additional acoustic stimulation: When acoustic stimulation increases the mean firing rate of a DCN PN above the target mean rate, homeostatic plasticity weakens excitatory synapses and strengthens inhibitory synapses. Therefore, immediately after switching off the additional acoustic stimulus, the spontaneous firing rate of the PN should be decreased. The spontaneous firing rate should then slowly recover to the value before the additional stimulation, but this process might take hours to days, as homeostatic plasticity has a rather long time constant.

To test the feasibility of additional acoustic stimulation against hyperactivity, we evaluate a generic case of noise-induced hearing loss with a threshold increase of 70 dB in the high-frequency range (Fig. 9a, top panel). We therefore employ a tonotopic array of AN fibers, WBI, NBI, and type III PNs organized in frequency channels, with characteristic frequencies from 1 to 8 kHz. To model the effects of noise-induced hearing loss, we adjust the degree of SD in each AN frequency channel such that the resulting response threshold of the AN fiber population matches the hearing threshold (compare Fig. 1b). This hearing loss leads to increased spontaneous firing rates of the affected type III PNs after homeostasis (Fig. 9a, bottom panel). The profile of hyperactivity has a peak, which occurs at the point of saturation of homeostasis at  $h = 3$  (Fig. 9a, middle panel). The characteristic frequency of the PN with the highest spontaneous firing rate is 4 kHz. If this profile is interpreted as the basis for a tone-like tinnitus sensation, its pitch would be 4 kHz.

We now evaluate the result of additional acoustic stimulation. Let us first consider a pure tone stimulus at 4 kHz with an intensity of 5 dB above the hearing threshold (Fig. 9b, top panel, dashed line). AN activity in this frequency channel is thus driven by the pure-tone stimulus unless a sound event with a higher intensity occurs in the acoustic environment (see also Methods). The mean firing rate of the AN fibers is increased by the additional acoustic stimulation, which also increases the activity of DCN PNs, but does not affect the inhibitory interneurons, because the stimulus is too soft. For prolonged stimulation, homeostatic plasticity adapts the PNs to this new input, and the homeostasis factor  $h$  is decreased in the stimulated PNs (Fig. 9b, middle panel). As a consequence, immediately after turning off the tone stimulus, the spontaneous firing rate of the DCN PNs in the 4 kHz channel is decreased (Fig. 9b, bottom panel, gray line). However, hyperactivity persists in the neighboring frequency channels that were not stimulated. Continuing with “no stimulation”, the pattern of spontaneous activity in the bottom panel of Figure 9b decays to the corresponding pattern in Figure 9a with the time constant of homeostatic changes.

Because patterns of spontaneous activity with peaks, as in the bottom panels of Fig. 9a and 9b, could underlie tinnitus, we demonstrate how a flat profile of spontaneous firing rates could be generated. More specific, using our model, we derive a stimulus that restores the spontaneous firing rates of type III PNs to their normal levels before hearing loss. By adjusting the intensities of an additional acoustic stimulus in all frequency channels in an iterative process, we find a matched-noise stimulus that achieves this goal (Fig. 9c, top panel, dashed line). The stimulus is a few dB above the hearing threshold in the high-frequency range where hearing is impaired. After prolonged stimulation with this stimulus, the homeostasis factors are reduced in the type III PNs (Fig. 9c, middle panel) compared to the situation before stimulation (Fig. 9a,

middle panel). During stimulation, the stimulus evokes firing rates around 90 Hz in the PNs (Fig. 9c, bottom panel, dashed line). After the stimulus is turned off, the profile of spontaneous firing rates of the type III PNs is flat along the tonotopic axis of the DCN (Fig. 9c, bottom panel, gray line). As homeostasis is a slow process, the re-emergence of hyperactivity (and thus tinnitus) might take hours to days.

## Discussion

We have implemented a phenomenological model of the basic DCN circuit (Young and Davis, 2002) to analyze how hearing loss through cochlear damage changes the response properties of projection neurons. Cochlear damage typically decreases the mean firing rates of AN fibers and DCN neurons. When the mean firing rate of a PN was stabilized in our model by homeostatic plasticity in response to decreased excitation from the AN, the resulting spontaneous firing rate depended on the response type of the PN (Fig. 7): hyperactivity occurred in type III and type IV-T PNs after OHC loss and SD. In type IV PNs, however, the spontaneous firing rates increased only little after OHC loss, and decreased after SD. In general, the development of hyperactivity in PNs through homeostasis is determined by the change of their ratio of mean and spontaneous firing rate induced by cochlear damage: hyperactivity develops only if this ratio is decreased, which is in line with our previous model with excitation only (Schäette and Kempter, 2006). The development of hyperactivity is a robust phenomenon if the healthy mean rate of a neuron is sufficiently above its spontaneous rate, i.e. when excitation in the input dominates over inhibition, like for example in type III and type IV-T PNs, but not in type IV PNs.

These modeling results are in line with seemingly contradicting experimental results on the spontaneous firing rates of DCN neurons in different species after acoustic trauma: In the chinchilla DCN, increased spontaneous firing rates were found in putative fusiform cells (Brozoski et al., 2002, anesthetized animals). Also in the hamster DCN, hyperactivity was strongest in the fusiform cell layer (Kaltenbach and Falzarano, 2002, anesthetized animals). In contrast, no indications of hyperactivity were found in principal cells of the cat DCN (Ma and Young, 2006, decerebrate preparation). Interestingly, also the prevalence of the different response types of DCN neurons seems to differ between species: In decerebrate cats, the majority of DCN PNs have been reported to possess type IV response characteristics (Young, 1980), whereas in anesthetized chinchillas the rate-intensity functions of DCN fusiform cells are more reminiscent of type III responses (Brozoski et al., 2002), similar to findings from decerebrate gerbils, where also type III responses were the most abundant (Davis et al., 1996b; Ding et al., 1999). Note however that results from decerebrate preparations and results that were obtained under anesthesia cannot be easily compared, as anesthesia may alter the response characteristics of DCN neurons (Young and Brownell, 1976). In our model, we found that DCN neurons with different response types differ in their aptitude for developing hyperactivity (Fig. 7), offering a putative explanation for diverse findings on hyperactivity in different animal species.

The amount of homeostatic compensation that is needed to give rise to hyperactivity in the model depends on the type of cochlear damage: After OHC loss, which does not change the spontaneous firing rates of AN fibers, even small increases in the strength of excitatory afferent synapses onto PNs lead to hyperactivity. After SD, which decreases the spontaneous firing rates of AN fibers, hyperactivity was observed in type III PNs when homeostasis increased the strength of excitatory synapses more than 1.6-fold, and in type IV PNs for more than 1.75-fold increases. These values are below the magnitude of homeostatic changes that have been seen, for example, in cultured cortical neurons with a 2.73-fold upregulation of mEPSCs size (Turrigiano et al., 1998) and a 1.7-fold increase in the slope of the f-I curve (Desai et al., 1999) after 48h activity blockade through TTX.

Changes that are reminiscent of homeostatic plasticity have been observed at various stages of the auditory pathway after hearing loss: In the auditory cortex of gerbils, bilateral cochlear

ablation elevated neuronal excitability, increased the amplitudes of evoked EPSCs, but decreased the amplitudes of evoked GABAergic inhibitory responses (Kotak et al., 2005). Similar changes were also observed in the inferior colliculus of gerbils, where bilateral deafening led to increased EPSC amplitudes and increased IPSC equilibrium potentials (Vale and Sanes, 2002). Increased EPSC amplitudes were also observed in the anteroventral cochlear nucleus of congenitally deaf mice in response to electrical stimulation of the AN (Oleskevich and Walmley, 2002). After unilateral ablation of the cochlea of guinea pigs, evoked glycine release (Suneja et al., 1998b) and glycine receptor binding (Suneja et al., 1998a) declined in the DCN, indicating weakened glycinergic inhibition. Furthermore, decreased expression of potassium channels was found in the cochlear nucleus (Holt et al., 2006) and the inferior colliculus (Cui et al., 2007) after bilateral cochlear ablation, indicating that the excitability of neurons in these nuclei might have been increased. Furthermore, the broadly tuned response maps of DCN neurons with mostly excitatory responses after acoustic trauma (Ma and Young, 2006) could also be explained by increased excitatory and decreased inhibitory synaptic strengths as a result of homeostatic plasticity.

In this study, we employed a model in which homeostasis was assumed to stabilize the mean firing rates of PNs only, whereas the activity of inhibitory interneurons was not regulated, and therefore their mean firing rates were decreased after cochlear damage. To test whether our results also hold without this restriction, we have also implemented a variant of the model where, in addition to the PNs, also the mean firing rates of the wide-band inhibitor (WBI) and the narrow-band inhibitor (NBI) neurons were stabilized by homeostatic plasticity (not shown). This, however, did not lead to hyperactivity in the WBI and NBI model neurons, regardless of the kind and severity of cochlear damage. In the PNs, on the other hand, hyperactivity was even slightly more pronounced: When homeostasis restores the mean activity of the inhibitory interneurons, inhibition in the PNs is increased, and thus even more homeostatic compensation is required to restore their mean firing rate, leading to stronger hyperactivity. Thus, in our model for the DCN, homeostasis in the inhibitory interneurons has only a minor quantitative, but not a qualitative influence on hyperactivity in PNs.

To compare our approach with other approaches on modeling the DCN, we note that the connectivity between AN fibers, inhibitory interneurons, and PNs in our model is motivated by the basic circuit that has been proposed for the DCN (Young and Davis, 2002). We could tune the PN responses to reproduce the rate-intensity functions of different response classes of DCN principal cells by varying the strength of the inhibitory projections from WBI and NBI neurons onto a PN (Fig. 4b-d). Reproducing salient response properties of DCN projection neurons, has also been the focus of several other modeling studies (Reed and Blum, 1995; Blum et al., 1995; Franosch et al., 2003; Zheng and Voigt, 2006a,b). Our model is similar to the model of Reed and Blum (1995), as it is also rate-based, whereas the more recent models of Franosch et al. (2003) and Zheng and Voigt (2006b) employ spiking neurons. Firing rates in our model represent average firing rates of small populations of real neurons.

A basic assumption in our model is that the responses of AN fibers from different frequency channels are mutually independent. While this might be reasonable for fibers whose characteristic frequencies are far apart, it might not be justified for nearby fibers with overlapping receptive fields. However, this assumption is important to analytically derive the response distributions and mean firing rates (Methods, Eqs. 6, 7, 9, 12, and 14). Alternatively, evaluating details of the correlations between frequency channels would force us to employ a detailed AN model and a large repertoire of naturalistic stimuli at different intensities. Cochlea and

hair cell models that capture the shape of the receptive fields of AN fibers would be necessary to reproduce the response maps of DCN neurons, the weak response of WBI neurons to pure tones (Young and Davis, 2002) and the nonmonotonicity of the rate-intensity functions of NBI (type II) neurons (Spirou et al., 1999). However, such detailed AN models that reproduce the effects of IHC loss, OHC loss, and SD are not yet available. Moreover, the exact choice of stimuli to represent the acoustic environment will also affect the results, and any conclusion drawn from such a model would rely on extensive numerical simulations only. The interpretation of such large-scale simulations is difficult without a solid analytical foundation, which we provide here in this article.

Another assumption in our model is that we included only type I AN fibers, which contact IHCs and constitute about 90-95% of all AN fibers. However, cochlear damage might also influence the activity of type II AN fibers which contact OHCs, and it has been suggested that reduced activity of type II AN fibers, for example after OHC loss, might be involved in the generation of DCN hyperactivity (Kaltenbach et al., 2002) and possibly also tinnitus (Jastreboff and Hazell, 1993): Reduced activity of type II AN fibers could influence DCN neurons via the parallel fiber system and lead to a disinhibition of PNs, thus increasing their spontaneous firing rates. This scenario could be implemented in our model by including an additional inhibitory input to the PNs, with the strength of inhibition reduced by OHC loss. This input would need to be spontaneously active so that its reduction can contribute to hyperactivity. However, as the responses and spontaneous firing rates of type II fibers *in vivo* have not been characterized yet (Robertson et al., 1999; Reid et al., 2004), we chose not to include them in our current model.

In the model presented in this study, the spontaneous activity of DCN projection neurons is driven only by the spontaneous firing of the afferent AN fibers. However, destruction of the cochlea does not abolish spontaneous activity in the DCN (Koerber et al., 1966; Zacharek et al., 2002), suggesting that the spontaneous firing of DCN neurons is also due to other sources. In addition to input from the ipsilateral AN, the DCN receives projections for example from the auditory cortex (Weedman and Ryugo, 1996) and the somatosensory system (Zhou and Shore, 2004). In our previous model, we have demonstrated that additional excitatory non-auditory input can be a source for the spontaneous activity of DCN neurons in the absence of input from the ipsilateral AN (Schaette and Kempster, 2006). Moreover, additional excitatory inputs typically boost the development of hyperactivity in this model (Schaette and Kempster, 2006), which corresponds to the experimental finding that additional inputs to the DCN can influence hyperactivity (Zhang et al., 2006). These findings on the effects of additional non-auditory excitatory inputs also apply to the model presented in this study, where additional inputs were omitted for simplicity, as they do not influence our main result that neurons with type IV response characteristics are less likely to become hyperactive than type III or type IV-T neurons.

A prediction of our model is that DCN hyperactivity could be reduced through additional acoustic stimulation (Fig. 9); the intensity of the optimal anti-hyperactivity stimulus is close to the hearing threshold, and the spectral shape of the optimal stimulus should be adapted to the hearing loss. Pure-tone stimulation (Fig. 9b) or white-noise-stimulation (Schaette and Kempster, 2006) might not be effective because the resulting patterns of spontaneous activity still have peaks. This prediction has direct implications for the treatment of tinnitus, which is related to hearing loss (König et al., 2006). Effective acoustic stimulation requires intact IHCs, thus hyperactivity induced by severe acoustic trauma that also leads to strong IHC loss may only be decreased by direct stimulation of the AN, for example through a cochlear implant

(Quaranta et al., 2004). Results that are similar to our prediction have been obtained from neurons in the auditory cortex of cats: exposure to an enhanced acoustic environment after acoustic trauma prevented the development of increased spontaneous firing rates (Noreña and Eggermont, 2005). Interestingly, also hyperacusis could be reduced through exposure to such an enhanced acoustic environment (Noreña and Chery-Croze, 2007), again demonstrating that neuronal response gain in the central auditory system of humans might be influenced by altered peripheral activity.

Another experimentally testable prediction of our model is that homeostatic plasticity in DCN neurons after hearing loss should lead to a higher percentage of monotonic rate-intensity functions compared to healthy DCN neurons (Fig. 6). Furthermore, the model predicts that isolated IHC loss, for example through carboplatin administration (Wang et al., 1997), should lead to less hyperactivity than OHC loss through cisplatin administration.

In summary, our results show under which conditions activity stabilization of neurons by homeostatic plasticity in response to changed input generates hyperactivity. The development of increased spontaneous firing rates depends on the relative strength and connectivity of excitatory and inhibitory inputs of a neuron and on the specific change of the statistics of the input signal.

## **Acknowledgments**

We would like to thank Christian Leibold for most helpful discussions on this work.

## **Grants**

This research was supported by the Deutsche Forschungsgemeinschaft (Emmy Noether Programm: Ke 788/1-3,4, SFB 618 “Theoretical Biology”, TP B3) and the Bundesministerium für Bildung und Forschung (Bernstein Center for Computational Neuroscience Berlin, 01GQ0410).

## **List of Abbreviations**

AN	auditory nerve
CF	characteristic frequency
DCN	dorsal cochlear nucleus
IHC	inner hair cell
NBI	narrow-band inhibitor
OHC	outer hair cell
PN	projection neuron
SD	stereocilia damage
WBI	wide-band inhibitor

# Bibliography

- J. J. Blum, M. C. Reed, and J. M. Davies. A computational model for signal processing by the dorsal cochlear nucleus. II. Responses to broadband and notch noise. *J. Acoust. Soc. Am.*, 98:181–191, 1995.
- T. J. Brozoski, C. A. Bauer, and D. M. Caspary. Elevated fusiform cell activity in the dorsal cochlear nucleus of chinchillas with psychophysical evidence of tinnitus. *J. Neurosci.*, 22:2383–2390, 2002.
- E. Christopher Kirk and D. W. Smith. Protection from acoustic trauma is not a primary function of the medial olivocochlear efferent system. *J. Assoc. Res. Otolaryngol.*, 4:445–465, 2003.
- Y. L. Cui, A. G. Holt, C. A. Lomax, and R. A. Altschuler. Deafness associated changes in two-pore domain potassium channels in the rat inferior colliculus. *Neuroscience*, 149:421–433, 2007.
- P. Dallos and D. Harris. Properties of auditory nerve responses in absence of outer hair cells. *J. Neurophysiol.*, 41:365–383, 1978.
- K. A. Davis, J. Ding, T. E. Benson, and H. F. Voigt. Response properties of units in the dorsal cochlear nucleus of unanesthetized decerebrate gerbils. *J. Neurophysiol.*, 75:1411–1431, 1996a.
- K. A. Davis, R. L. Miller, and E. D. Young. Effects of somatosensory and parallel-fiber stimulation on neurons in dorsal cochlear nucleus. *J. Neurophysiol.*, 76:3012–3024, 1996b.
- N. S. Desai, L. C. Rutherford, and G. G. Turrigiano. Plasticity in the intrinsic excitability of cortical pyramidal neurons. *Nat. Neurosci.*, 2:515–520, 1999.
- J. Ding, T. E. Benson, and H. F. Voigt. Acoustic and current-pulse responses of identified neurons in the dorsal cochlear nucleus of unanesthetized, decerebrate gerbils. *J. Neurophysiol.*, 82:3434–3457, 1999.
- M. A. Escabi, L. M. Miller, H. L. Read, and C. E. Schreiner. Naturalistic auditory contrast improves spectrotemporal coding in the cat inferior colliculus. *J. Neurosci.*, 23:11489–11504, 2003.
- J. M. P. Franosch, R. Kempter, H. Fastl, and J. L. van Hemmen. Zwicker tone illusion and noise reduction in the auditory system. *Phys. Rev. Lett.*, 90:178103, 2003.

- A. G. Holt, M. Asako, R. K. Duncan, C.A. Lomax, J. M. Juiz, and R. A. Altschuler. Deafness associated changes in expression of two-pore domain potassium channels in the rat cochlear nucleus. *Hear. Res.*, 216-217:146–153, 2006.
- P. J. Jastreboff and J. W. P. Hazell. A neurophysiological approach to tinnitus: clinical implications. *Br. J. Audiol.*, 27:7–17, 1993.
- J. A. Kaltenbach and P. R. Falzarano. DCN hyperactivity induced by previous intense sound exposure: origin with respect to cell layer. In *Assoc. Res. Otolaryngol. Abs.*, page 208, 2002.
- J. A. Kaltenbach and D. L. McCaslin. Increases in spontaneous activity in the dorsal cochlear nucleus following exposure to high intensity sound: a possible neural correlate for tinnitus. *Audit. Neurosci.*, 3:57–78, 1996.
- J. A. Kaltenbach and J. S. Zhang. Intense sound-induced plasticity in the dorsal cochlear nucleus of rats: evidence for cholinergic receptor upregulation. *Hear. Res.*, 226:232–243, 2007.
- J. A. Kaltenbach, J. M. Czaja, and C. R. Kaplan. Changes in the tonotopic map of the dorsal cochlear nucleus following induction of cochlear lesion by exposure to intense sound. *Hear. Res.*, 59:213–223, 1992.
- J. A. Kaltenbach, D. A. Godfrey, J. B. Neumann, D. L. McCaslin, C. E. Afman, and J. Zhang. Changes in spontaneous neural activity in the dorsal cochlear nucleus following exposure to intense sound: relation to threshold shift. *Hear. Res.*, 124:78–84, 1998.
- J. A. Kaltenbach, J. D. Rachel, T. A. Mathog, J. Zhang, P. R. Falzarano, and M. Lewandowski. Cisplatin-induced hyperactivity in the dorsal cochlear nucleus and its relation to outer hair cell loss: relevance to tinnitus. *J. Neurophysiol.*, 88:699–714, 2002.
- J. A. Kaltenbach, M. A. Zacharek, J. Zhang, and S. Frederick. Activity in the dorsal cochlear nucleus of hamsters previously tested for tinnitus following intense tone exposure. *Neurosci. Lett.*, 355:121–125, 2004.
- V. Kilman, M. C. W. van Rossum, and G. G. Turrigiano. Activity deprivation reduces miniature IPSC amplitude by decreasing the number of postsynaptic GABA<sub>A</sub> receptors clustered at neocortical synapses. *J. Neurosci.*, 22:1328–1337, 2002.
- K. C. Koerber, R. R. Pfeiffer, W. B. Warr, and N. Y. Kiang. Spontaneous spike discharges from single units in the cochlear nucleus after destruction of the cochlea. *Exp. Neurol.*, 16:119–130, 1966.
- O. König, R. Schaette, R. Kempfer, and M. Gross. Course of hearing loss and occurrence of tinnitus. *Hear. Res.*, 221:59–64, 2006.
- V. C. Kotak, S. Fujisawa, F. A. Lee, O. Karthikeyan, C. Aoki, and D. H. Sanes. Hearing loss raises excitability in the auditory cortex. *J. Neurosci.*, 25:3908–3918, 2005.
- S. Laughlin. A simple coding procedure enhances a neuron's information capacity. *Z. Naturforsch.*, 36:910–912, 1981.

- M. C. Liberman and L. W. Dodds. Single-neuron labeling and chronic cochlear pathology. II. Stereocilia damage and alterations of spontaneous discharge rates. *Hear. Res.*, 16:43–53, 1984.
- M. C. Liberman and N. Y. Kiang. Single-neuron labeling and chronic cochlear pathology. IV. Stereocilia damage and alterations in rate- and phase-level functions. *Hear. Res.*, 16:75–90, 1984.
- W. L. Ma and E. D. Young. Dorsal cochlear nucleus response properties following acoustic trauma: response maps and spontaneous activity. *Hear. Res.*, 216-217:176–188, 2006.
- W. L. Ma, H. Hidaka, and B. J. May. Spontaneous activity in the inferior colliculus of CBA/J mice after manipulations that induce tinnitus. *Hear. Res.*, 212:9–21, 2006.
- S. L. McFadden, C. Kasper, J. Ostrowski, D. Ding, and R. J. Salvi. Effects of inner hair cell loss on inferior colliculus evoked potential thresholds, amplitudes and forward masking functions in chinchillas. *Hear. Res.*, 120:121–132, 1998.
- A. J. Noreña and S. Chery-Croze. Enriched acoustic environment rescales auditory sensitivity. *Neuroreport*, 18:1251–1255, 2007.
- A. J. Noreña and J. J. Eggermont. Enriched acoustic environment after noise trauma reduces hearing loss and prevents cortical map reorganization. *J. Neurosci.*, 25:699–705, 2005.
- S. Oleskevich and B. Walmsley. Synaptic transmission in the auditory brainstem of normal and congenitally deaf mice. *J. Physiol.*, 540:447–455, 2002.
- N. Quaranta, S. Wagstaff, and D. M. Baguley. Tinnitus and cochlear implantation. *Int. J. Audiol.*, 43:245–251, 2004.
- M. C. Reed and J. J. Blum. A computational model for signal processing by the dorsal cochlear nucleus. I. Responses to pure tones. *J. Acoust. Soc. Am.*, 97:425–438, 1995.
- M. A. Reid, J. Flores-Otero, and R. L. Davis. Firing patterns of type-II spiral ganglion neurons *in vitro*. *J. Neurosci.*, 24:733–742, 2004.
- W. S. Rhode and S. Greenberg. Physiology of the cochlear nuclei. In A.N. Popper and R.R. Fay, editors, *The Mammalian Auditory Pathway: Neurophysiology*, chapter 3, pages 94–152. Springer, New York, 1992.
- D. Robertson, P. M. Sellick, and R. Patuzzi. The continuing search for outer hair cell afferents in the guinea pig spiral ganglion. *Hear. Res.*, 136:151–158, 1999.
- R. Schaette and R. Kempter. Development of tinnitus-related neuronal hyperactivity through homeostatic plasticity after hearing loss: a computational model. *Eur. J. Neurosci.*, 23:3124–3138, 2006.
- S. E. Shore. Multisensory integration in the dorsal cochlear nucleus: unit responses to acoustic and trigeminal ganglion stimulation. *Eur. J. Neurosci.*, 21:3334–3348, 2005.

- N. C. Singh and F. E. Theunissen. Modulation spectra of natural sounds and ethological theories of auditory processing. *J. Acoust. Soc. Am.*, 114:3394–3411, 2003.
- G. A. Spirou, K. A. Davis, I. Nelken, and E. D. Young. Spectral integration by type II interneurons in dorsal cochlear nucleus. *J. Neurophysiol.*, 82:648–663, 1999.
- S. K. Suneja, C. G. Benson, and S. J. Potashner. Glycine receptors in adult guinea pig brain stem auditory nuclei: regulation after unilateral cochlear ablation. *Exp. Neurol.*, 154:473–488, 1998a.
- S. K. Suneja, S. J. Potashner, and C. G. Benson. Plastic changes in glycine and GABA release and uptake in adult brain stem auditory nuclei after unilateral middle ear ossicle removal and cochlear ablation. *Exp. Neurol.*, 151:273–288, 1998b.
- G. G. Turrigiano. Homeostatic plasticity in neuronal networks: the more things change, the more they stay the same. *Trends Neurosci.*, 22:221–227, 1999.
- G. G. Turrigiano, K. R. Leslie, N. S. Desai, L. C. Rutherford, and S. B. Nelson. Activity-dependent scaling of quantal amplitude in neocortical neurons. *Nature*, 391:892–896, 1998.
- C. Vale and D. H. Sanes. The effect of bilateral deafness on excitatory and inhibitory synaptic strength in the inferior colliculus. *Eur. J. Neurosci.*, 16:2394–2404, 2002.
- J. Wang, N. L. Powers, P. Hofstetter, P. Trautwein, D. Ding, and R. Salvi. Effects of selective inner hair cell loss on auditory nerve fiber threshold, tuning and spontaneous and driven discharge rate. *Hear. Res.*, 107:67–82, 1997.
- Y. Wang, K. Hirose, and M. C. Liberman. Dynamics of noise-induced cellular injury and repair in the mouse cochlea. *J. Assoc. Res. Otolaryngol.*, 3:248–268, 2002.
- D. L. Weedman and D. K. Ryugo. Pyramidal cells in primary auditory cortex project to cochlear nucleus in rat. *Brain Res.*, 706:97–102, 1996.
- E. D. Young. Identification of response properties of ascending axons from dorsal cochlear nucleus. *Brain Res.*, 200:23–37, 1980.
- E. D. Young and W. E. Brownell. Responses to tones and noise of single cells in dorsal cochlear nucleus of unanesthetized cats. *J. Neurophysiol.*, 39:282–300, 1976.
- E. D. Young and K. A. Davis. Circuitry and function of the dorsal cochlear nucleus. In D. Oertel, R. R. Fay, and A. N. Popper, editors, *Integrative Functions in the Mammalian Auditory Pathway*, volume 15 of *Springer Handbook of Auditory Research*, chapter 5, pages 121–157. Springer, New York, 2002.
- M. A. Zacharek, J. A. Kaltenbach, T. A. Mathog, and J. Zhang. Effects of cochlear ablation on noise induced hyperactivity in the hamster dorsal cochlear nucleus: implications for the origin of noise induced tinnitus. *Hear. Res.*, 172:137–144, 2002.
- J. S. Zhang, J. A. Kaltenbach, Godfrey. D. A., and J. Wang. Origin of hyperactivity in the hamster dorsal cochlear nucleus following intense sound exposure. *J. Neurosci. Res.*, 84: 819–831, 2006.

- X. Zheng and H. F. Voigt. A modeling study of notch noise responses of type III units in the gerbil dorsal cochlear nucleus. *Ann. Biomed. Eng.*, 34:697–708, 2006a.
- X. Zheng and H. F. Voigt. Computational model of response maps in the dorsal cochlear nucleus. *Biol. Cybern.*, 95:233–242, 2006b.
- J. Zhou and S. Shore. Projections from the trigeminal nuclear complex to the cochlear nuclei: a retrograde and anterograde tracing study in the guinea pig. *J. Neurosci. Res.*, 78:901–907, 2004.

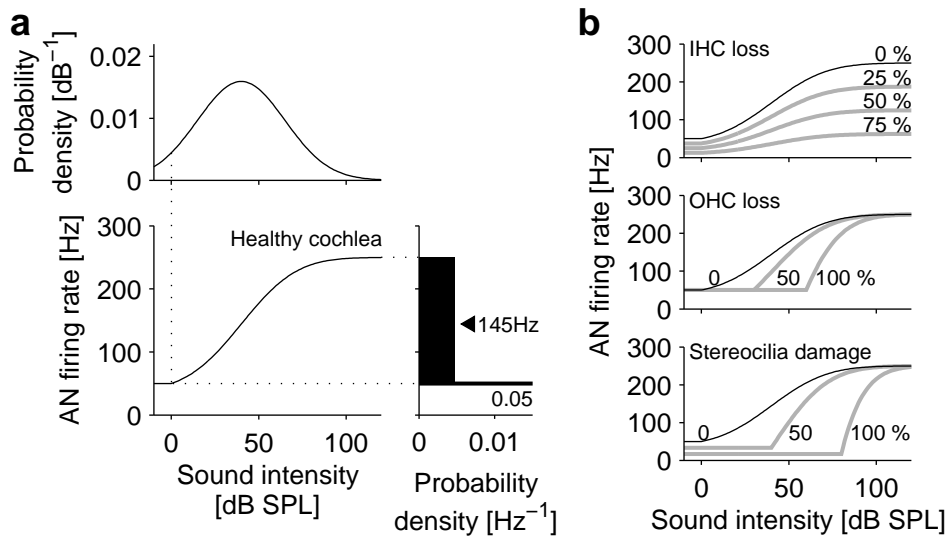


Figure 1: Auditory nerve (AN) model and hearing loss. **a**) Sound intensities in the acoustic environment are assumed to be Gaussian distributed (*top panel*) with a mean intensity of 40 dB and a standard deviation of 25 dB. The response of the AN (in each AN frequency channel) is described by an average firing rate of a small population of AN fibers (*central panel*). Given the acoustic environment and the AN rate-intensity function, the resulting distribution of AN firing rates (*right panel*) has a delta peak at 50 Hz, as spontaneous activity occurs with a probability of 0.05. The distribution of firing rate responses to super-threshold stimuli (black area) is flat, and the mean rate of the AN fiber population is 145 Hz. **b**) Hearing loss through damage to or loss of cochlear hair cells changes the AN population response. Loss of inner hair cells (IHCs, top panel) scales down the AN population response (0% IHC loss: black line; 25, 50, 75% loss: gray lines). Loss of outer hair cells (OHCs, middle panel) increases the response threshold (0% loss: black line; 50 and 100% loss: gray lines). Damage to the stereocilia of IHCs and OHCs (bottom panel) increases the response threshold and decreases the spontaneous firing rate of AN fibers (0% damage: black line; 50 and 100% damage: gray lines).

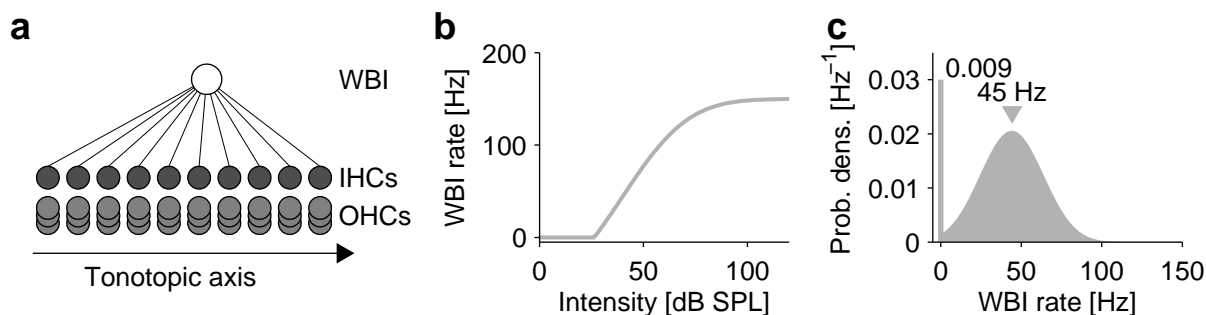


Figure 2: Wide-band inhibitor (WBI) model neuron. **a)** The WBI neuron is excited by the AN fibers of ten frequency channels (black lines) with a 2.5 octave range of characteristic frequencies. Inner (IHCs) and outer hair cells (OHCs) of the cochlea are depicted by circles. **b)** Rate-intensity function of the WBI neuron for stimulation with white noise. **c)** Firing-rate distribution of the WBI neuron. For AN input evoked by an idealized acoustic environment with a Gaussian distribution of sound intensities and independent frequency channels, the WBI neuron is inactive with probability 0.009 (delta-peak at 0 Hz), and has a mean rate of 45 Hz.

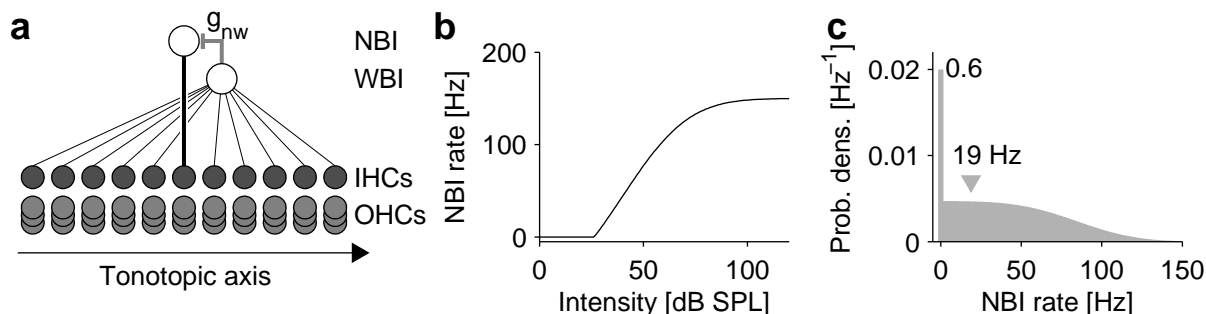


Figure 3: Narrow-band inhibitor (NBI) model neuron. **a)** The NBI neuron receives excitation from AN fibers of a single frequency channel (thick black line) and an inhibitory projection (thick gray line) from a WBI neuron with strength  $g_{nw}$ . The WBI neuron's receptive field is centered on the NBI neuron's characteristic frequency, but the two neurons are assumed to have no shared inputs to allow for a simple derivation of the response distributions. **b)** Rate-intensity function of the NBI neuron for stimulation with pure tones at its characteristic frequency. **c)** Firing-rate distribution of the NBI neuron for the idealized acoustic environment. The neuron is inactive with probability 0.6, and it has a mean rate of 19 Hz.

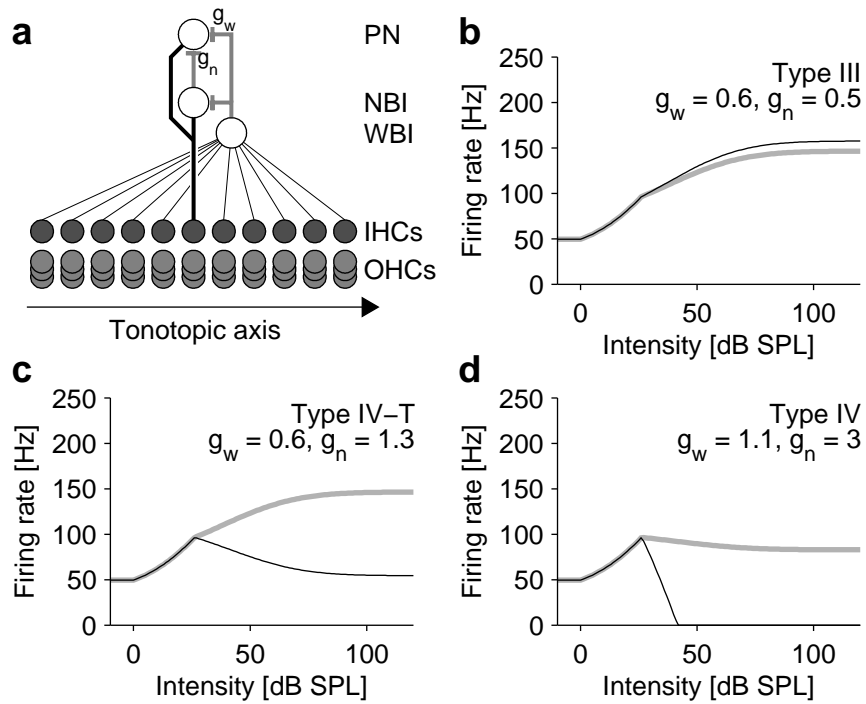


Figure 4: Model for a projection neuron (PN). **a**) The PN receives excitation from a population of AN fibers of a single AN frequency channel (thick black line), and inhibition from a NBI and a WBI neuron (gray lines). The strengths of the inhibitory inputs are determined by the respective gain factors  $g_n$  and  $g_w$ . The NBI neuron and the PN are excited by the same AN frequency channel, and they are inhibited by the same WBI neuron. **b,c,d**) Responses of the PN to pure tones (black lines) and broad-band noise (BBN, gray lines) for different combinations of  $g_n$  and  $g_w$  as indicated. At 27 dB intensity, the inhibitory interneurons start responding, leading to kinks in the PN rate-intensity functions. **b**) Type III response characteristics, i.e. excitatory responses to pure tones and BBN with monotonic rate-intensity functions. **c**) Type IV-T response characteristics, i.e. a nonmonotonic rate-intensity function for pure tones, and a monotonic rate-intensity function for BBN. **d**) Type IV response characteristics, i.e. nonmonotonic rate-intensity functions for pure tones and BBN.

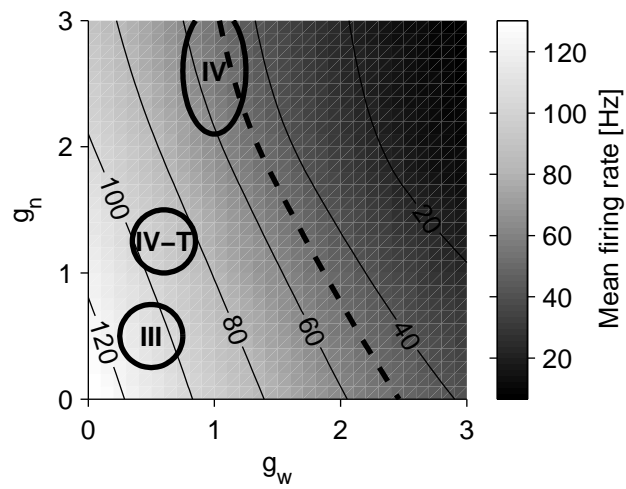


Figure 5: Mean firing rate of the model PN (gray level and the contour lines) in dependence upon the strength of narrow-band ( $g_n$ ) and wide-band ( $g_w$ ) inhibition. On the thick dashed contour line at 50 Hz the mean firing rate is equal to the spontaneous rate. The PN's mean rate decreases when  $g_w$  or  $g_n$  are increased. The black ovals show the parameter regions where type III, type IV-T, and type IV response properties are obtained.

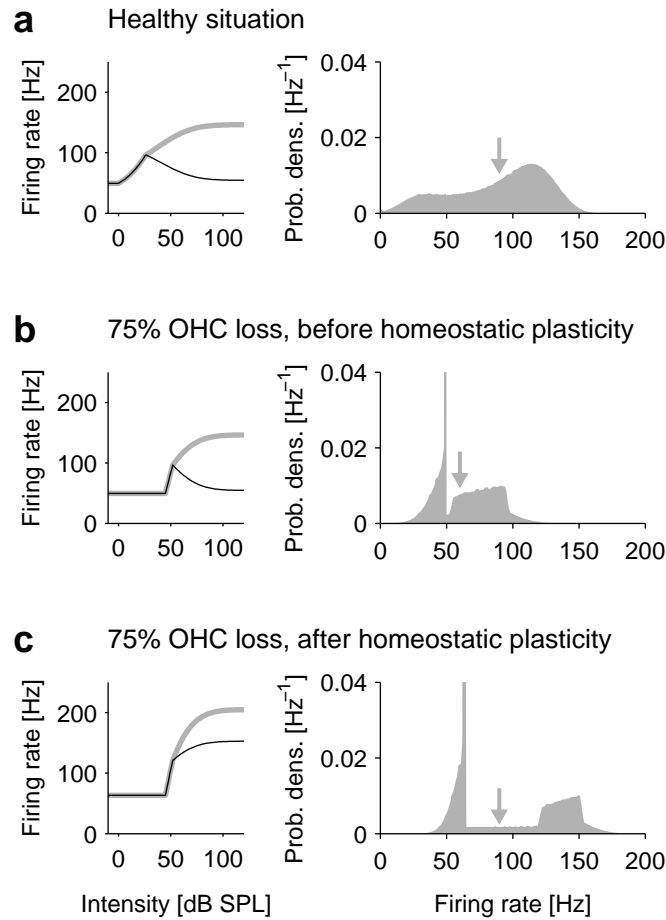


Figure 6: Development of hyperactivity through homeostatic plasticity in a type IV-T PN ( $g_w = 0.6$ ,  $g_n = 1.3$ ). The left column shows rate-intensity functions for pure tones (black lines) and BBN (gray lines). The right column depicts firing rate distributions (gray areas) for an acoustic environment with a Gaussian distribution of sound intensities in each frequency channel (see Fig. 1a), with mean firing rates indicated by arrows. **a)** Healthy situation. The type IV-T PN with a rate-intensity function as in Fig. 4c has a smooth firing rate distribution and a mean firing rate of 90 Hz. **b)** 75% OHC loss, before homeostatic plasticity. The response threshold of the PN is elevated, which increases the probability of spontaneous activity and leads to a pronounced peak in the firing rate distribution at 50 Hz. The mean firing rate is reduced from 90 to 60 Hz. **c)** 75% OHC loss, after homeostatic plasticity. To restore the mean firing rate to its value before OHC loss, homeostasis has increased excitatory synaptic strengths and decreased inhibitory synaptic strengths. As a consequence, the rate-intensity function for pure tones is now monotonic, the response distribution is bimodal, and the spontaneous firing rate is increased from 50 to 63 Hz.

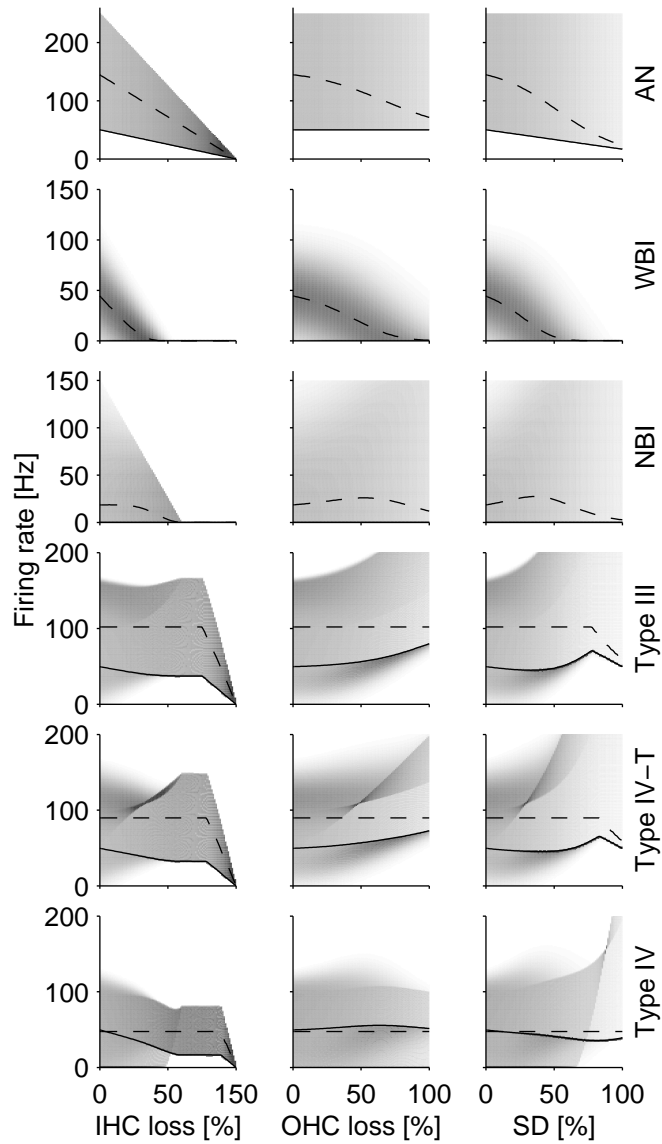


Figure 7: Distribution of firing rates as a function of the degree of IHC loss (left), OHC loss (middle), or SD (right) for AN fibers, WBI neurons, NBI neurons, and three different PNs (type III, type IV-T, type IV). PN responses are depicted after homeostatic plasticity. Mean firing rates are given by dashed lines, spontaneous firing rates by solid lines. The shaded areas indicate the distributions of firing rates, with the gray level representing the probability of occurrence of a specific firing rate.

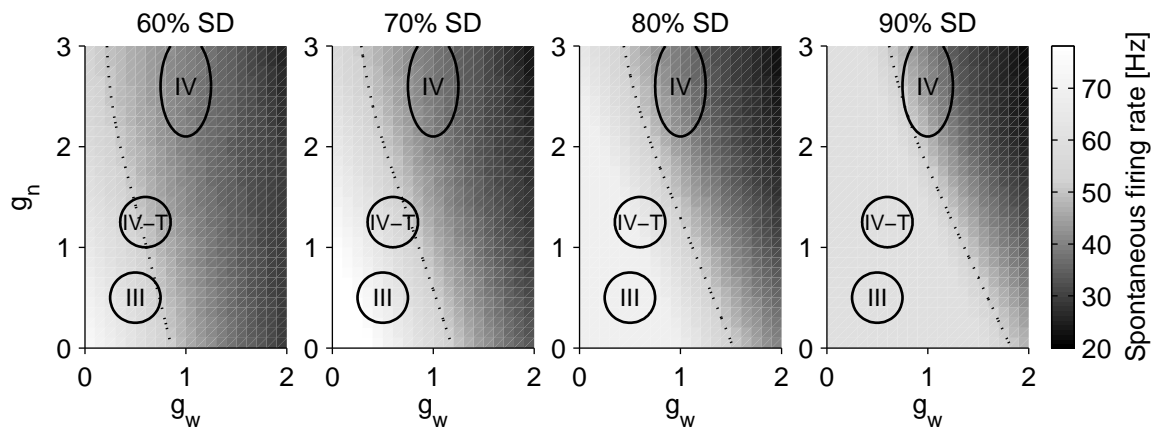


Figure 8: Spontaneous firing rates of PN neurons after SD and homeostasis as a function of the gain factors  $g_w$  and  $g_n$  of inhibitory inputs from the WBI and the NBI neuron, respectively. The spontaneous firing rates are depicted by the gray-scale levels. The dotted lines are at the spontaneous firing rate of 50 Hz, i.e. the healthy value before SD. Hyperactivity occurs below and to the left of the dotted line. The black ovals indicate the parameter regions where different response types of DCN neurons are observed. Four different degrees of SD are depicted.

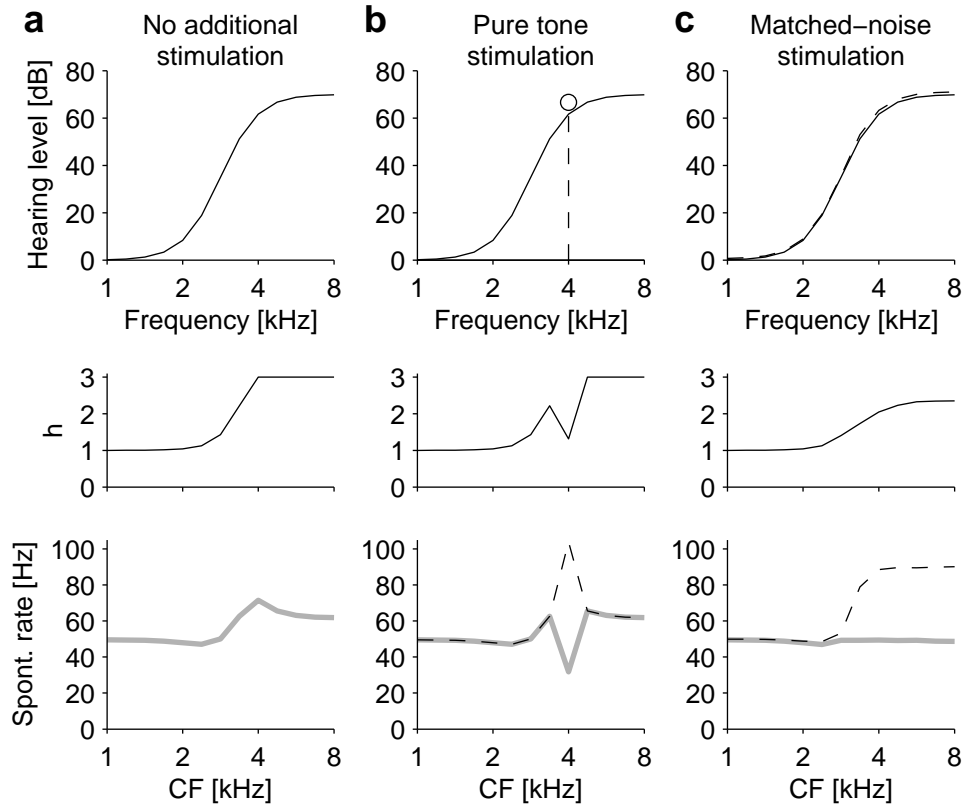


Figure 9: Impact of additional acoustic stimulation on spontaneous activity of a tonotopic array of DCN model neurons for a generic example of noise-induced hearing loss. The top panels show the hearing threshold curve (black lines), and levels of different acoustic stimuli (dashed lines). The three middle panels show the strength  $h$  of homeostatic plasticity in DCN type III PNs that are stimulated by AN input evoked by a mixture of ambient sounds and the additional acoustic stimulus (if applied). The bottom panels show the firing rate responses of type III PNs evoked during stimulation after homeostasis (dashed lines) as well as the spontaneous firing rates after stimulation (gray lines). **a**) No additional stimulation. After hearing loss and homeostasis, the spontaneous firing rates of DCN type III PNs are increased in the high-frequency range (gray line, bottom panel), with a peak at the characteristic frequency (CF) of 4 kHz. **b**) Stimulation with a 4 kHz tone at 5 dB above the threshold (dashed line, top panel) decreases the spontaneous firing rate of the corresponding type III neuron. **c**) Matched-noise stimulation adjusted for type III neurons. Immediately after stimulation, the profile of spontaneous firing rates is flat, the hyperactivity peak is gone.